Mine Water and the Environment (2021) 40:864–876
https://doi.org/10.1007/s10230-021-00825-8

TECHNICAL ARTICLE

Causes and Effects of a Water Spill from the Underground Pit of the Dashu Pyrite Mine, Southern Sichuan Basin, Southwest China

Bo Li[1,2,3] · **Guo Liu**[2,3,4] · **Yuhan Nie**[2,3,4] · **Zhong Ye**[2,3,4]

Received: 7 August 2020 / Accepted: 11 September 2021 / Published online: 26 September 2021

Abstract

In March 2019, a well was drilled in the north of the Dashu pyrite mining area in southwest China to extract shale gas from below the pyritic layer. This well passed through the karst water at the top of the Maokou Formation, leading to groundwater flowing into the pit in the north of the underground mining area and producing a large amount of acid mine drainage (AMD) by water-rock interactions with sulfur-bearing minerals. On Jan. 4, 2020, under the dual influence of progressive overpressure generated by water storage and AMD erosion, the underground pit's wall partially collapsed, resulting in over 280×10^3 m^3 of highly polluted AMD entering the Dashu River. About 231×10^3 kg of Fe, 171×10^3 kg of Al, 12×10^3 kg of Ni, and a large amount of other metals and trace elements were discharged. The main purpose of this study was to explain the causes, consequences, and effects of this event. Water and sediment samples were collected from the mine, the river, and the estuary, and a hydrological model of the underground pit was developed. The spill seriously affected the water quality of ≈16 km of the Dashu River. Given the low pH (≈2.5), most of the metals (Fe, Al, Mn, Cu, Zn, etc.) migrating towards the Dashu estuary were dissolved, but because of dilution and neutralization, much of the dissolved metals precipitated as river sediments, due to Fe and Al precipitation, and adsorption and co-precipitation of other metals. The calculated water balance and monitoring of the underground pit water levels show that the water in the pit mainly came from karst water recharge at the top of the Maokou Formation, increasing mine drainage by at least 17.2 m^3/h. Without effective action, serious environmental pollution or secondary geological disasters may occur in the future.

Keywords Dashu pyrite · Acid mine drainage · Underground pits · Environmental pollution

Introduction

Pyrite (FeS_2), a common symbiotic or associated metal sulfide mineral in coal and metal ore, is stable under reducing conditions. However, mining exposes FeS_2 to oxidation. Large amounts of FeS_2 may then be oxidized, releasing high concentrations of SO_4^{2-}, Fe, and other metal ions as acid mine drainage (AMD). Once these pollutants enter the environment, they can cause serious environmental pollution and ecological damage, and it can be difficult to control the pollution and restore the ecological environment. The prevention and control of AMD pollution is a worldwide problem (Bhattachary et al. 2012; Chen et al. 2012; Louis et al. 2015).

The Dashu pyrite is located in the Xuyong pyrite belt (XPB) in the southern Sichuan Basin (southwest China), a region that contains several large sulfide deposits (Duan 2017; Feng et al. 1999). It was once one of five pyrite production bases in China andhas caused serious environmental pollution occurred over its 100 years of mining history, especially during the 1970s, with large amounts of pollutants passing into the surrounding waters, including the perennial deposition of significant quantities of metal ions, causing the Dashu and Yongning Rivers to be severely contaminated (Zhou 2005; Zhao 2005).

✉ Bo Li
1063624529@qq.com

1 School of Environment and Resources, Southwest University of Science and Technology, Mianyang 621010, China

2 State Key Laboratory of Geohazard Prevention and Geoenvironment Protection, Chengdu 610059, China

3 State Environmental Protection Key Laboratory of Synergetic Control and Joint Remediation for Soil and Water Pollution SEKL-SW, Chengdu 610059, China

4 College of Environment and Ecology, Chengdu University of Technology, Chengdu 610059, China

In recent years, under the influence of national policies on resource integration, industrial restructuring, and environmental protection, most of these mines closed in 2002. However, to maintain the availability of the resource, the mines were not backfilled. Underground water levels rise rapidly after groundwater pumping stops and can enter inclined mine roadways, reacting with metal sulfide minerals to produce large quantities of AMD (Huang et al. 2016; Liu 2007;). Without preventive measures, contaminants can be released on a large scale, especially at abandoned mined areas, which typically have an adverse effect on the environment and human health (Olias et al. 2019; Rodrigues et al. 2016). Inclined mine roadway spills can occur because: (1) aquifers are damaged by human activity, causing groundwater recharge to increase; (2) acidic mine wastewater can weaken or even destroy a cement grout plug; or (3) the collapse of a mine structure and resulting hydraulic impact (Olias 2019; Younger 2002).

There are nearly a hundred abandoned pyrite and coal mines in the XPB, most of which continue to discharge acidic mine wastewater (Liu 2007; Zhao 2005). On Jan. 4, 2020, a sudden and unexpected spill occurred in the no. 2 mine in the central part of the Dashu pyrite mine, causing over 280,000 m^3 of AMD water to be spilled. This water quickly reached the Dashu River (Fig. 1), leading to serious water pollution, interrupting the water supply in Xuyong County, and causing a great deal of panic.

Accidental large-scale release of water from old pits have occurred in many locations. For example, Olias (2019) reported on the effects of the accidental release of the Iberian Pyrite Belt's La Zarza pit lake water on the Odiel River. Therefore, it is necessary to understand the causes of the spill from the Dashu pyrite mine, study its characteristics, and analyze the consequences and effects of the spill. The results of this study will have value for the analysis and prevention of similar accidents at poorly maintained abandoned mines throughout the world.

Research Area

The XPB is located at the bottom of the Permian Longtan Formation, at the southern margin of the Sichuan Basin, in southwest China. The Permian sequence contains layers of coal, sulfur, iron, aluminum, lead, and zinc (Li 1983; Li et al. 2015). The XPB is a typical volcaniclastic and weathered residual sedimentary deposit, with stable layers and coal-sulfur symbiosis as its main characteristics. The pyrite deposits are mainly characterized by a large number of massive and tuberculous sulfide deposits, which are mainly composed of pyrite (FeS_2), a small amount of chalcopyrite ($CuFeS_2$), Ni pyrite ($(Fe,Ni)_9S_8$), sphalerite (ZnS), and galenite (PbS) (Han and Niu 2010; Li 1992).

The Dashu pyrite mine is located in the middle of the XPB (Fig. 1). Topographically, the mining area is on higher elevation in the north and west, and lower in the south and east, ranging from ≈840 m in the north to 440 m in the south (Yang 1985). The region has a humid subtropical climate with an average annual precipitation of 1312 mm and an average temperature of 18 ℃. It is hot and rainy in summer and warm and humid in winter. The mining area is like a ridge, with a north–south length of 2.50 km and an

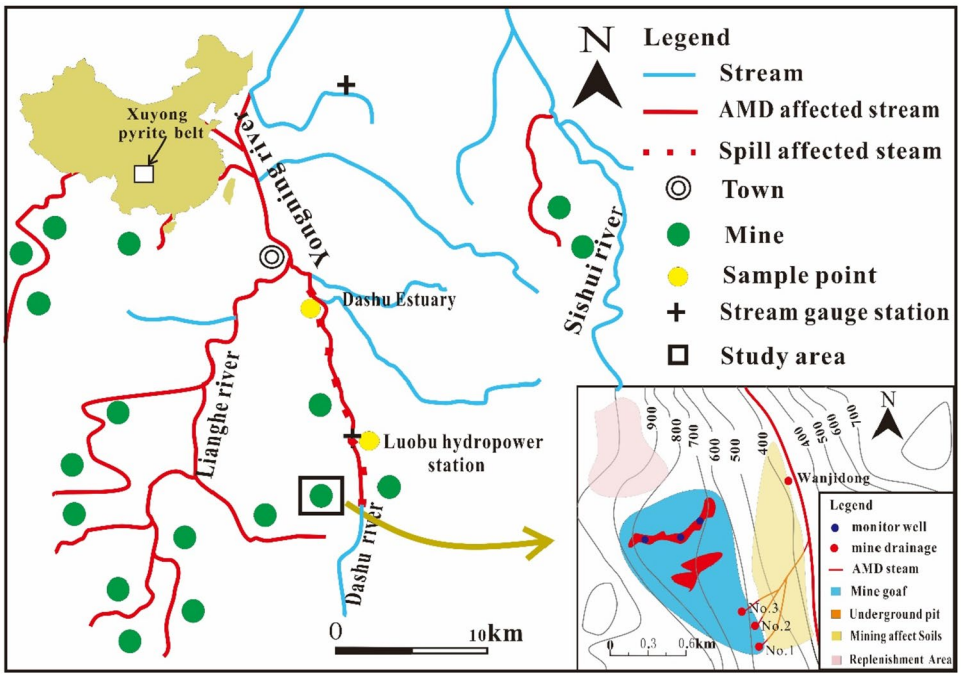

Fig. 1 Map of the Dashu River and the surrounding water system, indicating the area affected by the January 2020 spill, the sampling points (Luobu hydropower station and the Dashu estuary), and the Dashu pyrite mine area

average width of 0.23 m. The thickness of the pyrite layer is restricted by the paleosedimentary interface and changes with the palaeokarst erosion surface. The maximum mining thickness is 55 m, with an average between 5 and 15 m Gan 1985; He et al. 2004;).

The Dashu River is one of the main rivers flowing through the XPB, with a basin area of 322 km^2 and a total length of 19 km. About 1.6 km of the Dashu River flows through the mining area; the flow rate in the dry season is ≈0.60 m^3/s, but the maximum flow rate during the rainy season is ≈300 m^3/s.

The ores produced by the Dashu pyrite were mainly used to produce sulfur and sulfuric acid. The exploitation of these deposits began in the early 20th century, but large-scale development started in the 1960 s (He 2015). At first, mainly pyrite was mined, using blasting and other methods, which greatly increased the output, making it the largest pyrite mining and production enterprise in China, with an annual output of over 300,000 t of pyrite, and a cumulative output of > 10 million t (Gan 2019). Since 2002, pyrite mining has stopped, but the 2 m thick underground coal seam in the middle of the Longtan Formation is still being mined, using the backfill method. It is still the largest mining area in the XPB.

Subsequently, under the influence of national policies, most of the XPB mines were closed, including the Dashu pyrite mine. This also halted the pumping and discharging of groundwater from within the mining area, but the mines were not backfilled. Dashu pyrite carried out a comprehensive control of the mining environment in 2012, promoting the ecological restoration of the acidified soil in the formerly mined areas, with good results. The water quality of the Dashu River improved significantly, but less attention was paid to the mine water in the abandoned mining area, and the environmental pollution problem there was still very serious (He 2015).

Method

Hydrogeochemical Data

The day after the Jan. 4, 2020 underground pit spill, two monitoring stations were set up, one at the Luobu hydropower station, 3 km downstream of where the spill entered into the Dashu River, and one at the Dashu Estuary, and samples were collected two to three times a week (Fig. 1). As of Feb. 28, a total of 19 samples had been collected from the Luobu hydropower station site and 24 samples from the Dashu Estuary. Some samples were also collected further upstream and in other parts of the mining area. Portions of the collected samples were filtered with a 0.45 μm filter membrane, acidified with nitric acid to a pH < 2, and stored in a special organic sampling bottle. The samples were stored in an incubator at < 4 ℃ in the dark until analyzed. A second set of untreated samples (unfiltered, but acidified) were collected at the same time and stored in the same way to study the transport of metal particles caused by the spill, since the concentration differences between filtered and unfiltered samples may be due to particulate matter. The temperature, pH, electrical conductivity (EC), and oxidation-reduction potential (Eh) were measured using a portable HACH water quality analyzer with an accuracy of 0.01.

The collected samples were sent to the Sichuan Geological Engineering Survey Institute's Water Quality Analysis and Testing Center. Fe, Mn, Cu, Zn, and Al content were measured by inductively coupled plasma atomic emission spectroscopy, and Pb and Ni content was measured by inductively coupled plasma mass spectrometry. The detection limits were 0.001 mg/L and 0.07 mg/L, respectively. Ca and Mg were titrated with disodium ethylenediamine tetraacetic acid, with a detection limit of 1 mg/L. *N*, *N*-diethyl *p*-phenylenediamine spectrophotometry was used for determining sulfide content, with a detection limit of 0.005 mg/L. Fluoride was measured by ion chromatography with a detection limit of 0.02 mg/L. Other trace elements was analyzed by atomic fluorescence spectrometry, with a detection limit of 0.07 μg/L. The total dissolved solids were dried at 105 ℃ and then weighed.

The results of the water quality analysis of the mine drainage by Xuyong County Environmental Protection Bureau in June 2019 and Dec. 2019, as well as the results of water quality analysis of samples from Luobu hydropower station and Dashu River estuary collected in Dec. 2019, were used to establish the baseline conditions for the area before the spill, although only partial analysis were performed.

Dashu River Flow Data and Meteorological Information

The discharge and flow data for the Dashu River is from the Luobu hydropower station, located downstream from the mine (sampling point Luobu hydropower station, Fig. 1). Regarding the inflow of water into the underground pit, this is expressed as:

$$Q = 986.4 \times \alpha_1 \times W \times A_1 + 986.4 \times \alpha_2 \times W \times A_2, \quad (1)$$

where Q is the average water inflow into the underground pit (m^3/day), α_1 and α_2 represent the infiltration coefficients of atmospheric precipitation in the areas with and without soil cover in the replenishment area, W is the monthly cumulative precipitation (mm), and A_1 and A_2 are the areas of the replenishment zone with and without soil cover (km^2). A detailed description of the estimation process behind this relationship can be found in the report by He et al. (2019).

Water Level and Water Balance of the Underground Pit

To determine the change in the area of the underground pit that was inundated, the period from March 2019 to April 2020 were adopted, using the distribution map of the underground pit and goafs and the water level heights. In this way, the amount of water in the underground pit could be estimated by the groundwater level and the extent of the inundated surface of each orthographic projection (Fig. 2).

Through field surveys, it was found that the replenishment area is a limestone stratum with medium karst development and deep fractures in the northwest side of the mine (Fig. 1). The field surveys indicated that the precipitation infiltration coefficients for the areas without soil coverage and with soil coverage were 0.20 and 0.01, respectively (He et al. 2019). The maximum possible water input was estimated using formula (1).

Results and Discussion

Water Level Evolution of the Underground Pit

Due to the intensity of underground mining, a large area of goaf has formed in the mining area, along with two huge underground pits, similar to underground caves, the largest of which is located in the northern part of the mine area (600 m long, 110 m wide, and 50 m deep; Figs. 2 and 3). The underground pits are supported by concrete pillars that support the roof of the cave to prevent the collapse of the upper strata. After pyrite mining stopped in 2002, the mine stopped pumping water. To prevent groundwater from entering the underground pit and possibly causing disasters, cement walls were built at the entrance to the underground pits, and monitoring wells were set up to monitor the mine's water levels. The underground pit remained dry during most of March, but on March 24th, the drilling of shale-gas wells began at an altitude of 708 m, ≈ 30 m from the underground pit, to extract gas at a depth of ≈2500 m, and by 28 March, the drilling had reached 108 m. While drilling into the limestone formation at the top of the Maokou Formation, artesian groundwater erupted out of the drill pipe, reaching a height of 13 m above the ground. Instead of plugging the drill hole immediately, drilling continued to a depth of 138 m before the well was cased and cemented. Groundwater passed from the top of the inclined roadway of the Maokou Formation and was stored in the pit (Fig. 3). After that, the water from wells and springs north of the mine area decreased sharply until flow finally ceased.

The beginning of the water rise was observed on April 1 in the monitoring well west of the underground pit. A portable water level meter with a measurement error less than 1 cm was used for direct measurement; the number of measurements each time was not less than three and the average value was used as the measurement result. The water level of the underground pit rose rapidly and then gradually slowed during the following months (Fig. 4). In December, when the water level reached 582.05 m, it was speculated that it might have reached the edge of the undulating zone along the edge of the pit. This continued until January (Fig. 4), when the underground pit water body may have exceeded 600 m in length and 100 m in

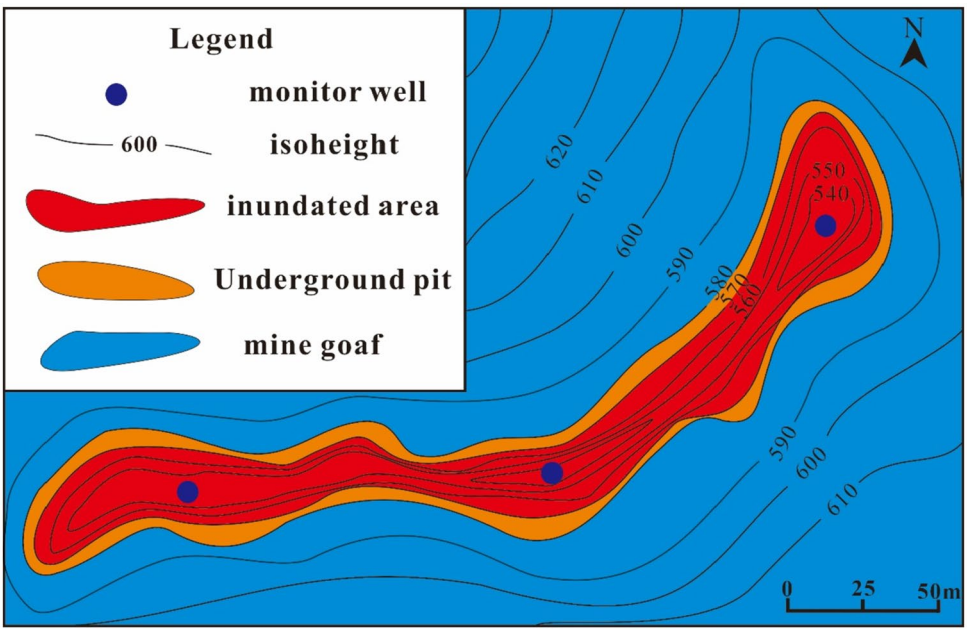

Fig. 2 Distribution diagram of underground pit and mined goaf area

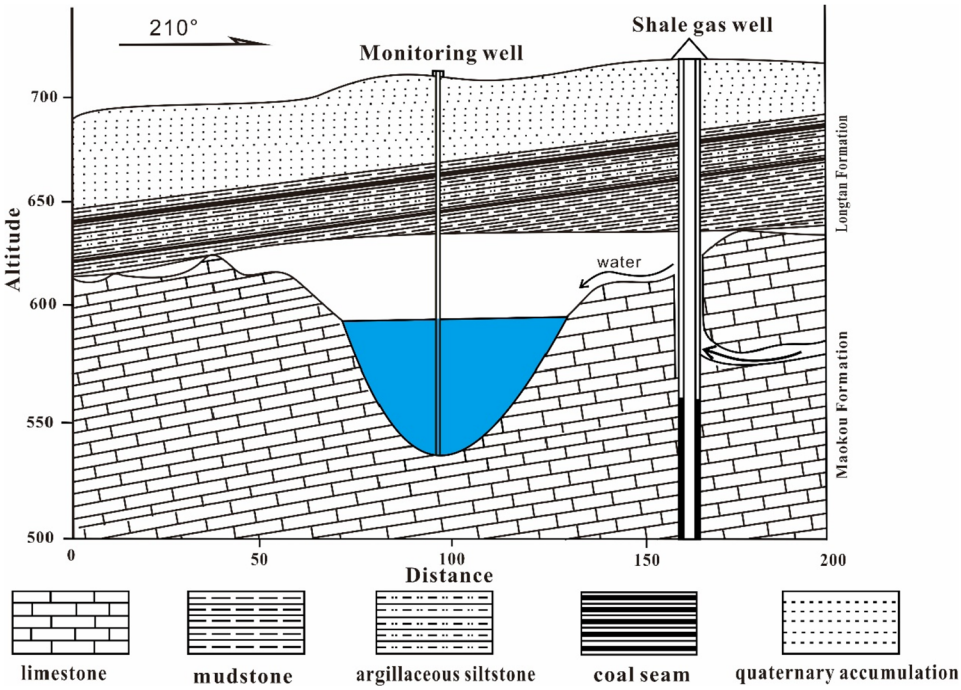

Fig. 3 Underground pit profile (the arrows indicate the direction of the water flow)

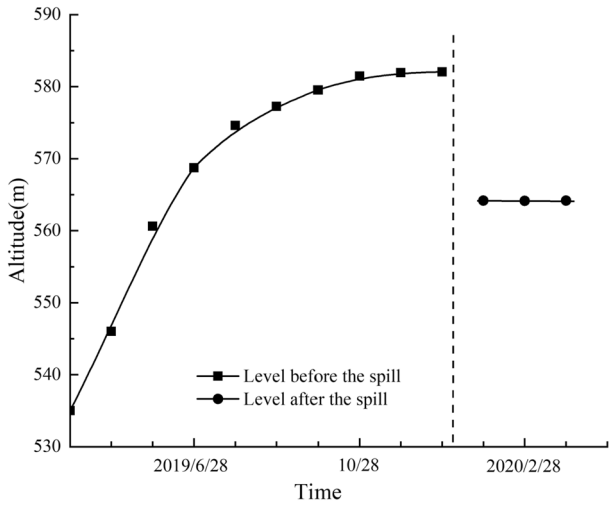

Fig. 4 Evolution of the water level in the underground mine over time as observed at the monitoring well west of the underground pit (the vertical dotted line indicates the date of the spill (January 4))

width (Figs. 2 and 3). On Jan. 4, 2020, the underground pit water level rapidly dropped and finally stabilized at a water level of 562.42 m.

The data presented in Fig. 4 shows that from March 2019 to January 2020, the underground pit water level rose ≈ 47 m, from 535.02 m in March to 582.05 m at the end of December (see Table 1), with an average monthly increase of 4.46 m. Under the dual influence of progressive overpressure generated by water storage and acidic water acting on the fractures in the limestone, causing dissolution at the top of the Maokou Formation, part of the mine's inclined roadway collapsed, and pit water began to spill.

Through hydrogeological analysis, it is found that the underground pit water is mainly supplied by atmospheric precipitation, and that changes in water volume are directly affected by atmospheric precipitation (Fig. 5). Water levels rose faster in the early stage of groundwater entering the pit (Fig. 4). In Nov. 2019, the underground pit's water level seemed stable. From Nov. 2019 to Dec. 2019, the pit water level only rose by 0.08 m. In Dec. 2019, the underground pit water storage was over 423×10^3 m^3 (Table 1). The total precipitation from April 2019 to Jan. 2020 was 1198 mm, with a monthly average of ≈ 119 mm, with May through September accounting for about 76% of the total.

Based on the underground pit's water levels in the monitoring wells, the inundated area can be estimated and determined using the mine goaf map (Fig. 2). It can be seen that the groundwater input increased with precipitation and the rate of the rise in the pit's water level slows with increasing inundated area and decreasing precipitation (Fig. 5).

The coal seams are mainly located in the lithologic mud shale, with a thickness of about 100 m, while the pyrite layer is mainly located atop the Maokou Formation. The permeability of the mud shales stratum is relatively poor and the amount of groundwater from this source was small during the mining process. Therefore, the underground pit water mainly comes from the average daily recharge of ≈ 1566 m^3/day of karst water at the top of the Maokou Formation and the water in the underground pit mainly comes from

Table 1 Groundwater pit water levels, water storage, supply, and mine water drainage data

Time	2019–04	2019–05	2019–06	2019–07	2019–08	2019–09	2019–10	2019–11	2019–12	2020–1
Level (m)	546.04	558.63	568.74	574.62	577.27	579.53	581.47	581.97	582.05	564.24
Precipitation (mm)	85.57	158.36	177.37	188.59	189.81	200.26	87.24	50.9	29.89	30.1
Inundated area (m^2)	2796	3715	4474	5485	6696	7898	8148	8347	8440	4054
V_{GR} (m^3)	30,994	57,359	64,244	68,308	68,750	72,535	31,599	18,436	10,826	10,902
V_{CGR} (m^3)	30,994	88,353	152,597	220,906	289,656	362,192	393,790	412,227	423,053	433,955
V_{IM} (m^3)	30,807	56,908	63,137	66,361	65,672	68,661	26,909	13,450	5028	0
V_{CIM} (m^3)	30,807	87,715	150,852	217,213	282,885	351,546	378,455	391,905	396,933	1,422,076
ΔV_1 (m^3)	187	451	1107	1948	3078	3875	4690	4986	5798	10,902
V_1 (m^3)	32,002	36,403	61,749	63,461	66,008	68,224	32,558	30,655	28,625	28,474
V_2 (m^3)	32,483	36,905	63,422	66,059	69,548	72,551	37,200	35,871	33,188	29,013
ΔV_2 (m^3)	481	3698	1673	2599	3541	4327	4612	5216	4563	481
ΔV_5 (m^3)	317	358	568	574	597	615	290	269	234	474
ΔV (m^3)	164	3340	1105	2025	2944	3712	4322	4947	4329	64

V_{GR} is the amount of groundwater recharge, and V_{CGR} is the cumulative groundwater recharge, V_{IM} increase of underground pit water, V_{CIM} represents the cumulative increase of water in underground mines, ΔV_1 represents the change in the total monthly drainage of the mine in 2019, V_1 and V_1 respectively, represent the monthly mine drainage in 2018/2019, ΔV_2 is the mine drainage water variation ($V_2 - V_1$), ΔV_5 represents the average change of mine drainage in the past 5 years, ΔV represents the increase in mine drainage ($\Delta V1 - \Delta V_5$), ΔV represents the cumulative increase in mine drainage

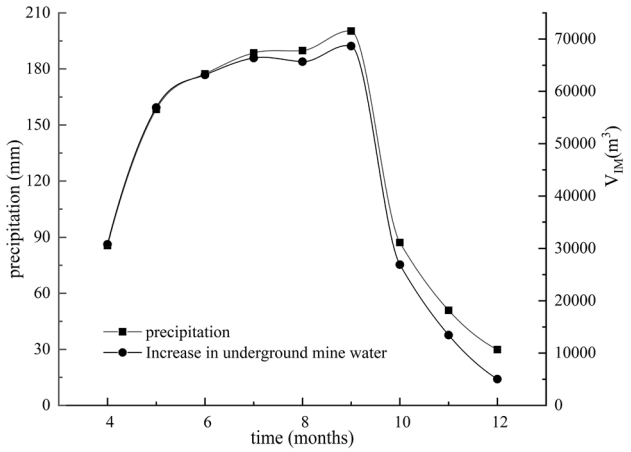

Fig. 5 The relationship between the increase in underground pit water volume and precipitation

infiltrated precipitation. According to the precipitation infiltration coefficient method (He et al. 2019), the water input was estimated to be slightly larger than the increment of the underground pit water. Some of the water may have entered the mine decline roadway through cracks and then flowed out of the mine mouth, since a significant increase in drainage was observed there. An analysis of the total monthly water drainage in the Dashu pyrite mine area over the past five years showed that the change in water drainage was less than 1%. The total monthly precipitation in 2018 and 2019 were similar, so we estimated the change in the total monthly drainage of the Dashu pyrite using the total drainage in 2019 minus the total drainage in 2018 to obtain ΔV_2. Then ΔV_2 was subtracted from the average mine drainage change during the past five years (ΔV_5) to get the underground pit's contribution to the total mine drainage ΔV (Table 1).

Table 1 shows that the difference (ΔV_1 of the last ninth row of Table 1) between the karst water recharge at the top of the Maokou Formation (V_{GR} in the fifth row of Table 1) and the underground pit storage increment of the underground pits (V_{IM} in the seventh row of Table 1) is close to the increment of the mine water drainage (ΔV of the last row of Table 1; Fig. 4), which means that there was no other significant water volume input. Since April 2019, the water storage of the underground pit has been continuously increasing. By the end of December, the accumulated water volume of the underground pit was about 423×10^3 m^3. However, the difference between the underground pit recharge and pit water gradually increased (Fig. 6). Compared with November and before, the increase in underground pit water in December was only 5028 m^3, which was close to the increase in total mine drainage of 4329 m^3. This shows that the accumulated water in the underground pit may have reached the pit's edge. The total amount of water outflow from the mine increased by 25,342 m^3 (about 6% of the input). This water may discharge via poorly blocked mine roadways and from the inclined roadway through mining-induced fractures.

The upper strata of goaf in the Dashu pyrite mine are mainly mudstone, argillaceous siltstone, coal seams, and Quaternary accumulation deposits (Fig. 3), with a permeability of about 10^{-9} m/s, which indicates that very little of this groundwater can penetrate to the underground pits (Yan et al. 2019). This confirms that the water entering the pit mainly comes from karst water at the top of the limestone

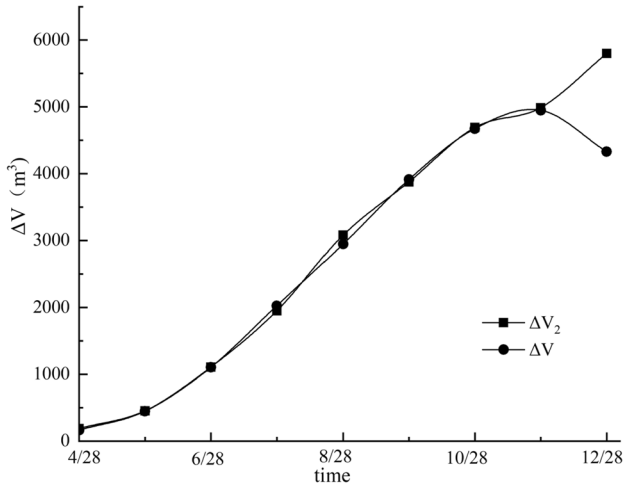

Fig. 6 Comparison chart of water volume change trend (ΔV_2 represents the karst water replenishment of the Maokou Formation minus the increase of underground mine

of the Maokou Formation and is replenished by infiltrating precipitation. According to the field measurements, the recharge area is about 1.83 km^2 (Fig. 1).

After October, the water level rise slowed down (Fig. 4), which was mainly due to three factors: (1) the inundated area increases as the water level rises because of the shape of the opening (Fig. 3), which causes the water level increase rate to slow down, even if the amount of water supplied is the same; (2) after October, the mining area entered the dry season, which decreased groundwater replenishment to the underground pit (Fig. 5), and; (3) as the pit water level rose, water discharged from the pit through mining-induced fractures into the roadway (Fig. 6). Depending on precipitation, the amount of pit water should be equal to the amount of groundwater inflow minus the water outflow. Balancing this amount of water required increasing the amount of water in the underground pit by the amount discharged during the spill. According to Table 1, assuming that the water infiltrating from precipitation was 423,053 m^3 in Dec. 2019, the inundated area of the underground pit must have reached 8846 m^2, equivalent to a height of 47.82 m, which is 47.03 m higher than the water level observed in the monitoring wells in Dec. 2019 (Fig. 4). This is lower than the expected equilibrium water level, probably due to the mining-induced rock fractures around the pit; hydrological balance may be reached in the future (Liu et al. 2007). However, the mine is located in the limestone stratum at the top of the paleokarst development of the Maokou Formation, and the acidic water reacts with the limestone fractures, thus increasing the width of the fractures. When the fracture width has increased to a certain extent, it may collapse under the action of water pressure and lead to a dramatic release, similar to the La Zarza pit lake spill (Olias et al. 2019). To avoid environmental pollution from the spillage of AMD, it is necessary to carry out detailed hydrogeological studies and take appropriate control measures.

Basic Conditions Before the Spill

The Dashu pyrite mine has formed a huge goaf underground after nearly a century of mining activities, with an area of about 3.26 km^2. Several waterways discharge AMD from the mine eastwards, which are collected by a ditch and flow into the Dashu River (Fig. 1). Even at high flow rates, the pH of the ditch was below 3.00, with the concentration of various elements being 390 to 492 mg/L for Fe, 451 to 711 mg/L for Al, and 4.9 to 14.9 mg/L for Mn (see Table 2). After the mine was closed, no effective measures were taken to prevent AMD from forming and flowing out of the three main Dashu pyrite mines, of which the no. 2 mine had the largest amount of water. According to the Xuyong County Environmental Protection Bureau, the total outflow from the mine was about 60 m^3/h, and the water contained 297 to 1450 mg/L of Fe, 216 to 787 mg/L of Al, 9.9 to 14.7 mg/L

Table 2 Analytical results for the mine water drainage, Dashu estuary, and spill water of the Dashu pyrite mine

Sampling site	Sampling time	Test item								
		pH	Fe (mg/L)	Al (mg/L)	Mn (mg/L)	Zn (mg/L)	Cu (mg/L)	Ni (μg/L)	F (mg/L)	SO_4^{2-} (mg/L)
No. 1 mine	2019–12	2.17	1450	216	10.4	5.94	1.02	4.08	4.81	81,300
	2019–06	2.57	955	273	9.94	5.09	0.85	5.01	1.36	11,400
No. 2 mine	2019–12	2.08	829	665	12.4	5.48	2.00	3.51	2.84	10,300
	2019–06	2.27	553	497	9.69	4.68	1.59	4.63	5.59	10,800
No. 3 mine	2019–12	2.05	525	787	14.7	3.95	1.45	2.38	2.17	14,800
	2019–06	2.66	297	445	10.5	3.10	1.22	2.98	5.54	10,300
Mine drainage	2019–12	2.22	492	711	14.9	3.84	1.56	2.75	1.67	12,500
	2019–06	2.63	390	453	4.94	1.52	0.53	4.26	3.80	34,200
Dashu estuary	2019–12	7.08	0.03	0.06	0.10	0.02	0.02	3.84	0.19	46
Spill water	2020–01	2.53	826	612	13.7	5.43	1.54	4.37	3.57	16,380

of Mn, and Ni, Cu, Zn, and Fl concentrations < 10 mg/L, Table 2). According to the monitoring data collected in 2019, the Dashu River pollutant load was about 3430 kg/day for Fe, 2750 kg/day of Al, and 54.5 kg/day of Mn, with the Dashu mine being one of the main contributors.

Also, the AMD discharging from different mines along the Dashu River will affect the river's water quality. The pH value of the river water in areas unaffected by the AMD can reach 8.2, as groundwater recharges the river. The acidic substances in the AMD neutralize the limestone fragments that accumulate in the river and the slightly alkaline river water. Under the dual effects of neutralization and dilution, the pH value increases and some metal ions precipitate, thus playing a certain self-purification role. Therefore, the pH of the lower reaches of the Dashu River is ≈6.8, with a SO_4^{2-} concentration of ≈50 mg/L, and Fe, Cu, Mn, Ni, and Zn concentrations < 1 mg/L (Table 2).

The Spill in January, 2020

On Jan. 4, 2020, under the dual effects of gradual pressure from the stored underground pit water and corrosion by the acidic water, the limestone around the pit ruptured. More than 280×10^3 m^3, equivalent to two-thirds of the water in the pit, discharged. The water released contained high concentrations of pollutants, such as 826 mg/L of Fe, 612 mg/L of Al, 13.7 mg/L of Mn, and 3.6 mg/L of fluoride, which are similar to the levels in the previous drainage water from the mine (Table 2), though at a lower pH. The total contaminant concentrations (dissolved and particulate) was not similar to that of the dissolved, with only the dissolved concentrations shown in Table 2.

As the spill happened suddenly, no timely and effective measures could be taken to collect and treat the spilled water, and so all of it entered the river. Compared with the annual pollution load of the Dashu River, except for Fe, Al, and Mn, which are 8.86%, 6.89%, and 14.50% of the annual load, respectively (Table 2), the effect of the spill was relatively small (increasing pollutants by ≈1.6%). Also, compared with other such accidents around the world, the pollution caused by the Dashu mine spill was not especially serious. For example, at the La Zarza pit lake in Spain, 220,000 m^3 of AMD (2,883 mg/L of Fe, 624 mg/L of Al, and 6.75 mg/L of As) was released after a concrete plug ruptured in the Los Cepos mine roadway, polluting about 50 km of river (Olias et al. 2019).

The water did not contain extremely high contaminant concentrations. This was mainly due to the significant increase in particulate matter and suspended material produced by erosion of the Dashu pyrite, which causes most metals to migrate in the particle/colloidal phase, which is less dangerous to living organisms. The spill did not cause extremely high pollutant concentrations in the river. The neutralization reaction between limestone fragments in the river and the AMD as well as the dilution effect of the river water, to some extent mitigated the effect of the spill. Also, most of the metals migrated in the particle/colloidal phase, so no fish deaths or adverse effects on the aquatic ecosystems were observed after the spill. Although the amount of water released by this spill was larger than that from the La Zarza pit, the concentrations and load of pollutants in the Dashu river were much less.

A similar incident occurred at the Gold King mine (Colorado, United States), where a spill was caused by the rupture of an unconsolidated wall, leading to the release of 113,000 m^3 of AMD stored in an underground roadway, polluting about 550 km of the San Juan River (Rodriguez et al. 2016). The spilled water had a high concentration of iron and manganese ions and was dark red, which after flowing into the surrounding waters, changed the color of the river and caused great public concern. Therefore, under the special fund support of the Xuyong government and the Ministry of Ecology and Environment, the Dashu pyrite comprehensive pollution control project began in March 2020, with the aim of adopting a long-term solution to control the pollution there.

Effect on the Dashu River

The spill affected 16 km of the Dashu River. These pollutants entered the river (Fig. 1), causing serious pollution and abrupt color changes in the river, leading to panic among the local residents and the emergency interruption of water supplies in Xuyong County. As mentioned above, the water flow of the Dashu River is small in winter, and the AMD had a serious impact on the water quality of the river. The aquatic ecosystem is characterized by the absence of mollusks and other higher organisms. The presence of life in these waters, especially during the dry season, is limited to eosinophilic microorganisms, and therefore, despite the release of large amounts of pollutants, the underground pit spill had little effect on the aquatic ecosystems. Similar findings were observed in the La Zarza pit water spill in Spain (Olias et al. 2019).

As the spill occurred during the dry season, the flow of the Dashu River was low and dilution was reduced. However, because there is a tremendous amount of limestone deposited in the riverbed, and the river is mainly recharged by karst water, the river waters' pH is relatively high, which is conducive to its neutralization reaction with the spilled AMD. This caused some of the metal ions to precipitate, reducing the seriousness of the spill's influence on the river water quality. The sampling point of Luobu Hydropower Station 3 km downstream of the Dashu pyrite mine, the flow rate was 0.62 m^3/s on Jan. 4, and increased to 1.84 m^3/s a day

later. After that, the flow rate decreased, and was less than 0.80 m^3/s on Jan. 9 (Fig. 7a).

The spillover effect is demonstrated by the significant decrease in the river water's pH values and increase in the EC and Eh values observed at the Luobu hydropower station and the Dashu estuary (Fig. 6b–d). Also, the Dashu River turned dark red on Jan. 4, visually distinct from the section upstream of the spill. High concentrations of contaminants such as Fe, Al, and Mn were observed in the samples collected on Jan. 5, demonstrating this effect (Fig. 7a–c). The concentration of dissolved pollutants peaked on Jan. 5, with Fe at 525 mg/L, Al at 345 mg/L, and Mn at 8.2 mg/L, which were much higher than the usual ion concentrations at the Luobu hydropower station, which are usually about 0.38 mg/L for Al, and between 0.02 and 0.2 mg/L for Fe, Cu, Mn, and Zn (Fig. 8). From Jan. 13 onwards, the metal/colloid concentrations at the Luobu hydropower station sampling point dropped rapidly.

The increase of pollutant concentrations at the Dashu River estuary is shown in Fig. 8. It should be noted that: (1) during the dry season, the Dashu River has less flow due to less run off, and less potential for dilution and neutralization of pollutants; (2) due to the cold winters, rainfall is relatively low, and a trend of increasing concentrations is usually observed in the rivers of this region. Fe and Al do not follow this trend, and the concentrations kept decreasing (Fig. 8a, b). This was mainly due to the neutralization and dilution already discussed, and because Fe and Al precipitate after hydrolysis.

The pollution loads of the dissolved elements at the Luobu hydropower station on Jan. 4 and 18 were estimated based on the flow and analytical data. There was some lack of hydrochemical information, given the failure to take samples immediately after the spill, so these estimates assume that the concentrations on the day of the spill were similar to those on Jan. 5, though based

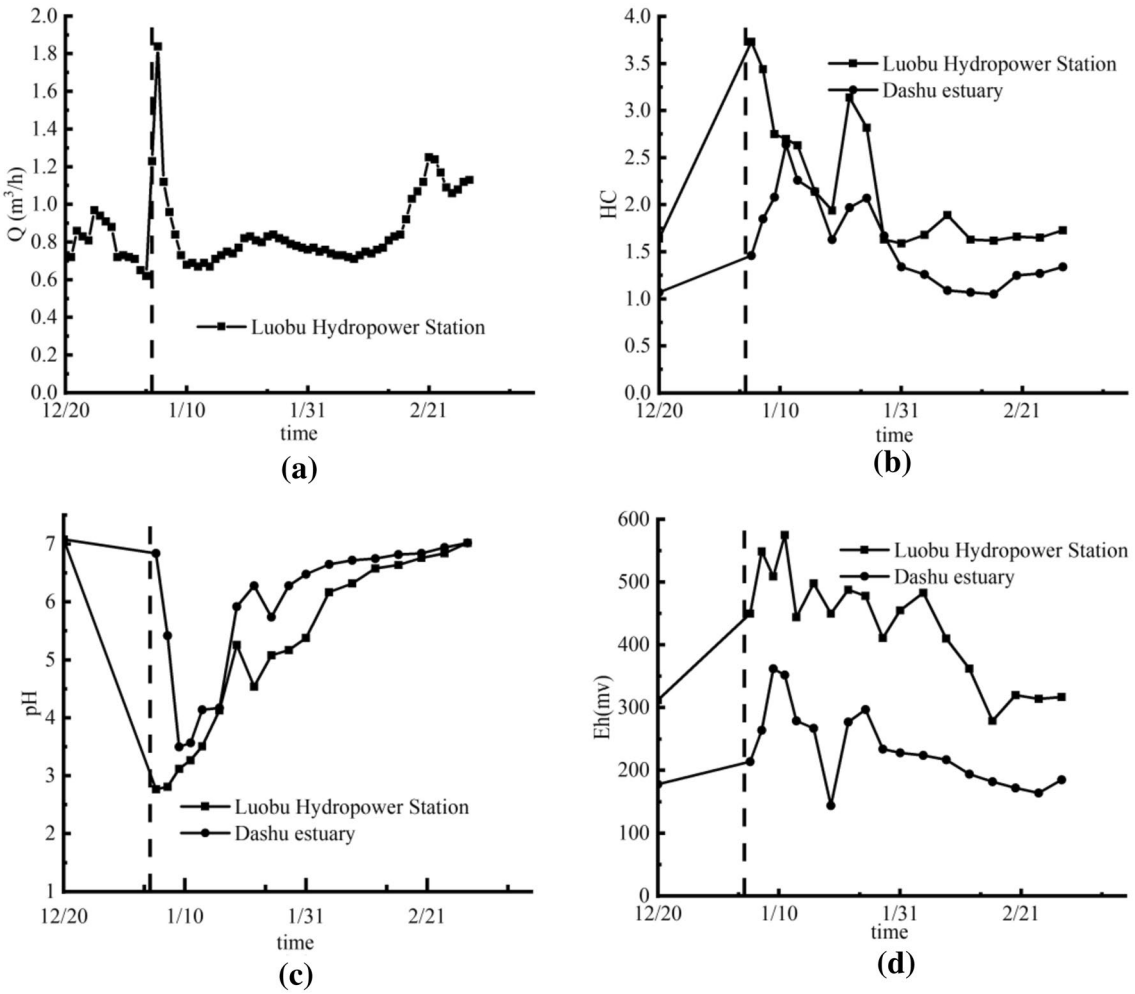

Fig. 7 Evolution of pH, Eh, and EC levels at the Luobu hydropower station and the Dashu estuary and the flow at the Luobu Hydropower station (see Fig. 1). The vertical dotted line indicates the date of the spill (January 4)

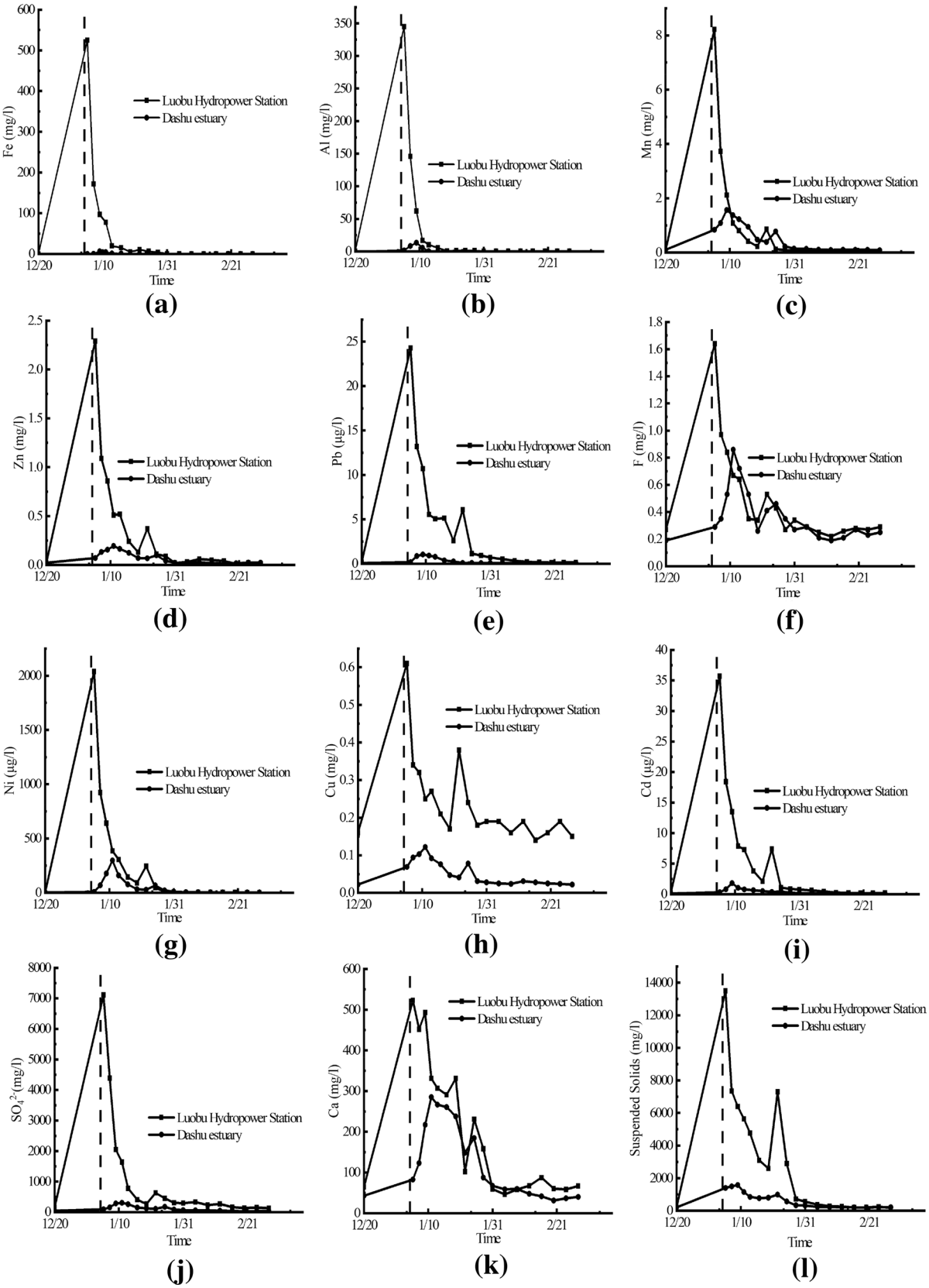

Fig. 8 Changes in the concentration of certain elements in the Dashu River (sampling sites at the Luobu hydropower station and the Dashu estuary). The vertical dotted line indicates the date of the spill (January 4)

on the trend observed on Jan. 5, the actual value of the elemental pollution load estimated by the Luobu hydropower station measurements may be too low. The release concentrations of Fe, Al, Mn, Ni, and other pollutants in the river increased by at least 50–884 times due to the spill (Table 2). Most of the Fe and Al released from the underground pit (about 86 and 76%) reached the upstream reach of the Luobu hydropower station, though much precipitated in the Dashu River drainage network, along with adsorbed and co-precipitated trace elements, especially during the dry season (Table 3).

Low levels of river flow caused the contaminated plume to flow slowly in the river before reaching the estuary (Fig. 1). The maximum concentration of most elements was reached one week after the spill, and the effect lasted until Feb.14 (Fig. 8). For most elements, the maximum concentration observed at the Dashu River estuary was about 21% less than the maximum concentration observed at the Luobu hydropower station, and the plume was flatter due to dispersal, with results similar to those of Gandolfi et al. (2001) regarding hydrodynamic dispersion for river water quality. However, compared with the values at the Luobu hydropower station, the maximum Fe and Al concentrations decreased by more than 98.8%, mainly because these metals precipitated. The peak concentrations of Zn, Cd, and Pd were all observed to decrease by more than 90% between the two sampling sites (Zn by 93%, Cd by 95%, Pb by 95%,).

Although there has been no significant increase in metal ions in the estuary (Fig. 8), the maximum ion concentrations of Mn and fluoride at the Luobu hydropower station and the Dashu estuary showed less of a drop than the other ions (Fig. 7c, f). These values may have been influenced by other AMD sources between these two sampling points, particularly those associated with Wanjidong point, which typically account for 18–32% of the total pollutants in the region. Redissolution and/or desorption processes may also occur in the sediments, which can affect the concentrations of certain elements.

Impact on the Dashu Estuary

No aquatic deaths or other effects on the aquatic ecosystem were observed after the spill. On Jan. 18, river sediment samples were collected 1 and 0.5 km upstream of the estuary, and 0.5 and 1 km downstream of the estuary, as well as at the leakage point and the Luobu hydropower station sampling point (Table 3). The pH values of the sediments in the estuary were between 3.1 and 8.2, and the contents of Fe, Al, Mn, and Ni were 20.30×10^3 mg/kg, 3.12×10^3 mg/kg, 36.50 mg/kg, and 10.60 mg /kg, respectively. Because of the neutralization reactions between the limestone fragments and the AMD in the river, as well as the dilution and neutralization effect of the river, the pH at the estuary was close to neutral (the estuary pH was 6.5, Fig. 7c). Most of the Fe was retained in the river by co-precipitation/adsorption, so the metal concentrations in the river decreased significantly (Fig. 8a).

Like the Dashu River, the estuary has suffered from AMD contamination for a long time. The concentrations of toxic elements in the estuary depends on the pollutants in the river and the effects of mixing with the more alkaline Yongning River. To analyze this effect, AMD elements were sampled in the main sediments of the river system (Table 3). The content of Fe, Al, Ni, Mn, and other elements in the Dashu river system sediments decreases along the flow direction of the river, with the Fe, Al, Mn, and Ni content at the estuary being between 2 and 30 times higher than downstream of the estuary. The decrease in metal ions in the river and stream sediments at the estuary is mainly due to dilution and neutralization by the river water, while the increase in pH causes some metal ions (mainly Fe and Al) to settle before reaching the estuary. Although large amounts of metals and metal oxides were released, the effects of the spill appear to be limited to the upper reaches of the estuary. A similar situation was observed at the Wheal Jane mine leak, considered the most serious in the UK, and at the La Zarza pit lake in Spain (Banks et al. 1997; Olías et al. 2019). Dealing with water pollution from Kernow to Kwauzulu Natal, Younger

Table 3 Test results from the river sediment analyses

Sampling site	Test item (mg/kg)											
	Fe	Mn	Al	Ni	Ba	Be	Cr	Co	Pb	Zn	Cu	Cd
Mine water spill area	323×10^3	225.0	71.1×10^3	395.00	250.00	10.90	315.00	332.0	61.5	385.0	166.0	3.74
Luobu hydropower station	251×10^3	112.0	29.3×10^3	106.00	187.00	3.73	119.00	59.1	36.4	157.0	131.0	1.54
1 km upstream of estuary	284×10^3	81.0	6.78×10^3	41.60	64.50	1.62	34.20	23.5	9.7	43.8	48.2	0.35
0.5 km upstream of estuary	7.01×10^3	49.1	4.01×10^3	36.80	36.60	0.87	24.30	17.0	6.4	37.9	28.4	0.19
Estuary	2.03×10^3	36.5	3.12×10^3	18.80	15.20	0.62	11.50	9.1	4.8	15.7	16.6	0.15
0.5 km downstream of the estuary	0.99×10^3	16.2	0.60×10^3	7.13	8.30	0.12	8.10	5.4	1.7	5.5	8.9	0.10
1 km downstream of the estuary	0.70×10^3	6.17	0.29×10^3	2.06	4.50	0.04	3.60	2.5	1.1	2.6	2.8	0.06

The detected concentrations of As, Se, Ti, Tl, Mo, B, and Hg were less than 1 mg/kg, so they have not been included in the table

(2002) attributed this phenomenon to density differences between the AMD and estuarine waters, as well as the fact that dilution and neutralization of pollutants in many estuarine waters prevented benthos from absorbing the pollutants.

Summary and Conclusions

The accidental spill from the Dashu pyrite underground pit resulted in the release of about 280,000 m^3 of acidic water with high concentrations of metal ions into the Dashu River: about 231×10^3 kg of Fe, 171×10^3 kg of Al, 12×10^3 kg of Ni, and a large amount of other metals and trace elements. The spill contaminated 16 km of the river and severely affected the water quality of rivers and estuaries, making it the worst water pollution incident in the region since the mine closed nearly a decade ago. The concentration of some pollutants in the river increased by nearly a hundredfold. Because of the dry season, the maximum flow in the drainage period was 1.84 m^3/s, which is significantly greater than the river flow before the spill, but it declined rapidly. As a result, the plume moved slowly along the river, with the peak reaching the estuary within a week of the spill. Spillover effects lead to a 15- to 200-fold increase in the concentration of metals in the upper part of the estuary, with less effect in the lower estuary, similar to what has been observed in other studies.

Analysis of the evolutionary process of the underground pit flood shows that the underground pit has reached a hydrological balance. Since the water of the underground pit is mainly recharged by karst water from the top of the limestone stratum of the Lower Maokou Formation, the drainage water of the Dashu pyrite no. 2 mine can increase by at least 17 m^3/h, and by 100 m^3/h in the wet period, which will greatly increase the challenge of avoiding continued seasonal environmental pollution. There are nearly a hundred mines of different sizes in the XPB, more than half of which have different degrees of water outflow, and most of which were forced to close due to national policies at the end of the 20th /early 21st centuries. Future studies should focus on monitoring the effects of mine water pollutants on the estuarine biota. Because of the large amount of AMD, a case-by-case study of these systems is urgently needed to assess the risk of mine water outflow and to take the necessary precautions. There needs to be a detailed survey of the distribution and hydrogeology of old mining projects to clarify the relationship between the recharge, runoff, and discharge of the mine water, and to provide scientific guidance for the prevention and control of such polluting waters.

Acknowledgements This work was supported by State Key Laboratory of Geohazard Prevention and Geoenvironment Protection Independent Research Project (SKLGP2019Z008) and the Special Fund for Environmental Protection of China. Thanks to the Xuyong County Environmental Protection Bureau and Chuankan Group for their great help in the sampling and analysis test.

References

Banks D, Younger PL, Arnesen R-T, Iversen ER, Banks SB (1997) Mine water chemistry: the good, the bad, and the ugly. Environ Geol 32:157–174. https://doi.org/10.1007/s002540050204

Bhattachary P, Scraek O, Eldvall B, Asklund R, Barmen G, Jacks G (2012) Hydrogechemical study on the contamination of water resources in a part of water resources in a part of Tarkwa mining area, western Ghana. Afr Earth Sci 66:72–84. https://doi.org/10.1016/j.jafrearsci.2012.03.005

Chen YT, Li JT, Chen LX, Hua ZS, Huang LN, Liu J, Xu BB, Liao B, Shu WS (2012) Biogeochemical processes governing natural pyrite oxidation and release of acid metalliferous drainage. Environ Sci Technol 48(10):5537–5554. https://doi.org/10.1021/es500154z

Duan PP (2017) Geochemical characteristics of harmful elements in high-sulfur coal in southwest China and their distribution by washing. PhD Diss, China University of Mining and Technology **(In Chinese)**

Feng XB, Hong B, Ni JY, Hong YT (1999) Chemical activity of some potentially toxic trace elements in coal under supergenic conditions. J Environ Sci 19(4):433–437. https://doi.org/10.3321/j.issn:0253-2468.1999.04.017 (**In Chinese**)

Gan CX (1985) Type of ore deposits and prospecting direction in the southwest sulfur belt. Chem Geol 3:1–2. CNKI:SUN:HGKC.0.1985-03-000 (**In Chinese**)

Gan Y, Wang C, Cheng Y (2019) Study on the Occurrence law of geothermal resources in the red zone of the central and western Sichuan Basin. J Groundw 41(2):41–45. https://doi.org/10.3969/j.issn.1004-1184.2019.02.012 (**In Chinese**)

Gandolfi C, Facchi A, Whelan MJ (2001) On the relative role of hydrodynamic dispersion for river water quality. Water Resour Res 37:2365–2375. https://doi.org/10.1029/2001WR000249

Han P, Niu G (2010) Discussion on the main concentration areas and resource potential of sulfur deposits in China. J Chem Min Geol 32(2):95–103. CNKI:SUN:HGKC.0.2010-02-006 (**In Chinese**)

He B, Wang YM, Jiang XW (2004) Determination of paleokarst landform on the top of limestone of Maokou Formation. China Geol J 1:50–55 (**In Chinese**)

He LH, Liu JH, Li LB, Xu WD (2019) Estimation of groundwater recharge in northern Xingguo County. Resour Environ Eng 33(1):79–83 (**In Chinese**)

He MY (2015) Overview of geological and environmental management of pyrite mine in Lubo Area, Xuyong County. In: Academic exchange meeting on coalfield geology. https://doi.org/10.3969/j.issn.1006-0995.2014.z2.048 **(In Chinese)**

Huang JY, Qin M, Yu J, Peng XJ, Yang L (2016) Characteristics analysis and ecological risk assessment of heavy metal pollution in river suspended solids affected by acidic mine wastewater. J Environ Chem 35(11):2315–2326. https://doi.org/10.7524/j.issn.0254-6108.2016.11.2016032501 (**In Chinese**)

Li R (1983) Characteristics and enrichment law of pyrite in south Sichuan. J Chem Min Technol S1:5–8 (**In Chinese**)

Li Z (1992) Classification and distribution of sulfur deposits in China. J Guizhou Chem Ind 1:13–16. CNKI:SUN:GZHG.0.1992-01-002 (**In Chinese**)

Liu JY, Zhao YJ (2007) Environmental pollution problems and control countermeasures in the mining and utilization of pyrite resources. J China Min Ind 16(7):55–57. https://doi.org/10.3969/j.issn.1004-4051.2007.07.017 (**in Chinese**)

Liu PG, Shu LC, Wang X, Tao YZ (2007) Analysis on the influence of mine drainage on the water supply safety of groundwater source. J Hydrol 27(5):55–57. https://doi.org/10.3969/j.issn.1000-0852.2007.05.014 (**In Chinese**)

Li YZ, Xu CH, Wu XY (2015) Analysis on ore characteristics and mineralization of pyrite in Xulong etuary, Sichuan. China Non Met Miner Ind Guide 1:46–49. https://doi.org/10.3969/j.issn.1007-9386.2015.01.016 (**In Chinese**)

Olias M, Canovas CR, Basallote MD, Macias F, Perez-Lopez R, Moreno Gonzalez R, Millan-Becerro R, Nieto JM (2019) Causes and impacts of a mine water spill from an acidic pit lake (Iberian pyrite belt). Environ Pollut 250:127–136. https://doi.org/10.1016/j.envpol.2019.04.011

Louis A, Yu H, Shumlas SL, Aken B, Strongin DR (2015) Effect of phospholipid on pyrite oxidation and microbial communities under simulated acid mine drainage (AMD) conditions. Environ Sci Technol 49(13):7701–7708. https://doi.org/10.1021/es505374g

Rodriguez-freire L, Avasarala S, Ali A, Agnew D, Hoover JH, Artyushkova K (2016) Post Gold King Mine spill investigation of metal stability in water and sediments of the Animas River watershed. Environ Sci Technol 50(21):11539–11548. https://doi.org/10.1021/acs.est.6b03092

Yang S (1985) Variation characteristics and exploration pattern analysis of Dashu coal-measure pyrite ore body in Sichuan. J Chem Miner Geol 32(1):47–52. CNKI:SUN:HGKC.0.1985-01-005 (**In Chinese**)

Yan NG, Chengfeng W, Yixi C (2019) Study on the occurrence law of geothermal resources in the red Zone of the Central and Western Sichuan Basin [J]. J Groundwater 41(02):41–45. CNKI:SUN:DXSU.0.2019-02-013 (**In Chinese**)

Younger PL (2002) Mine water pollution from Kernow to Kwauzulu Natal: geochemical remedial options and their selection in practice. Geosci SW Engl 10:255–266

Zhao Yongkang (2005) Worrying Yongning river. J Green China Public Edn 8:19–21 (**In Chinese**)

Zhou Yu (2005) The sadness of a river—the injury and pain of the Yongning River wine city. J Green China Public Edn 8:12–18 (**In Chinese**)